Chemical Physics Letters 636 (2015) 203–207

Contents lists available at ScienceDirect

Chemical Physics Letters

journal homepage: www.elsevier.com/locate/cplett

Non-Faraday rotation of the free induction decay in gaseous NO

E.N. Chesnokov[a,*], V.V. Kubarev[b,c], P.V. Koshlyakov[a], Y.V. Getmanov[b], O.A. Shevchenko[b,c]

[a] Institute of Chemical Kinetics and Combustion, Novosibirsk 630090, Russia
[b] Budker Institute of Nuclear Physics, Novosibirsk 630090, Russia
[c] Novosibirsk State University, Novosibirsk 630090, Russia

ARTICLE INFO

Article history:
Received 26 May 2015
In final form 18 July 2015
Available online 29 July 2015

ABSTRACT

Effect of rotation of the polarization plane of free induction decay in magnetic field is observed. Experiments were performed using short pulse of terahertz Free Electron Laser in the region of pure rotation transitions of NO molecule. Rotation of polarization was observed in real time using ultra-fast Schottky diode detectors. Angle of rotation depends on time after the laser pulse and exceeds 180° in field <1 kG. Observed effect could be used in time-domain spectroscopy for the selection of the free induction decay of paramagnetic species.

1. Introduction

When a short optical pulse creates a coherent superposition of two energy levels, this nonstationary state emits radiation that continues as long as phase coherence exists. This effect is the well-known optical free induction decay – FID [1]. If the optical pulse excites many absorption lines, FID becomes more diverse due to the interference of many emitters [2]. The FID signal contains complete information about the spectrum of the absorbing medium. Magnetic field can affect the FID signal in two ways. First, because of the Zeeman splitting of the absorption lines, the number of different emitter increases. This should cause an additional modulation of the FID. Such modulation of the FID in external electric field was observed in [3]. And second, magnetic field can change the polarization of the FID.

A longitudinal magnetic field can rotate the polarization plane of the FID. The physical nature for this rotation is that the absorption lines for right- and left-hand circular polarization become different. A similar effect was observed in experiments with photon echo [4] that was called 'non-Faraday rotation'. It was shown that the rotation angle of photon echo increases with time after the exciting pulse. Photon echo and FID are closely related effects. Simply speaking, the photon echo is the FID which cannot be observed directly due to inhomogeneous broadening and which therefore requires special techniques [5]. Based on this, one can expect a similar dependence of the rotation angle of the FID on time. Therefore, for long-duration FID signals [6] the rotation angle can be large.

The effect of rotation of the polarization plane in longitudinal magnetic field is often used to isolate lines of paramagnetic molecules from the non-magnetic component. Faraday rotation spectroscopy based on cw-lasers is often used for the sensitive and selective detection of paramagnetic molecules or radicals in the gas phase [7]. It utilizes the fact that the absorption frequency of radicals is tunable with an external magnetic field and optical circular dichroism arises in the longitudinal magnetic field. Most often this technique is used in the mid-IR range of vibration-rotation spectra to detect such molecules as NO [7–12], NO_2 [13–15] C_2H [16], OH [17,18]. Also it was used in the range of electronic transitions for O_2 [19,20] and NO_2 [21] detection and in the pure rotation spectra of OH and NO [22].

All studies with cw-lasers use the influence of the external magnetic field on molecular spectra in the frequency domain. In this letter we report the first experimental observation of the effect of rotation of the plane of FID polarization in the magnetic field that should be regarded as the influence on molecular spectra in the time domain. It should be stressed that in contrast with conventional Faraday effect, which is typically very small, the rotation of polarization of the FID is large. In our experiments the angle of rotation reaches 180° in magnetic field <1 kG. Therefore the observed effect is a promising approach in time-domain spectroscopy to isolate the spectra of paramagnetic species.

2. Experimental

Experiments were performed on Novosibirsk Free Electron Laser (NovoFEL) [23]. This laser is continuously tunable in the range 45–88 cm^{-1} with a spectral width of 0.2 cm^{-1}. It emits a sequence of pulses at repetition frequency of 5.6 MHz with the energy of 5–20 μJ

* Corresponding author.
E-mail address: chesnok@kinetics.nsc.ru (E.N. Chesnokov).

http://dx.doi.org/10.1016/j.cplett.2015.07.043
0009-2614/

and duration of 100–150 ps. The laser beam is linearly polarized; polarization is horizontal. The laser radiation passed through the gas sample in the magnetic field to the detector. Self-made ultrafast Schottky diode detectors with the resolution <30 ps were used [24]. Signals were accumulated by a 30 GHz LeCroy digital oscilloscope. Before entering the sample, a small fraction of the laser beam was reflected by a flat 30 μm polypropylene film to the second Schottky diode detector, which was used to trigger the oscilloscope.

The sample was in the cylindrical gas cell 35 cm long, 4 cm in diameter, fitted with polypropylene windows. The cell was mounted inside the solenoid. The magnetic field was varied within 0–720 G. The magnetic field inhomogeneity along the cell was ±20%.

The polarizer was placed after the gas cell in order to monitor with the detector only vertical polarization. The polarizer attenuates horizontal polarization on the detector by a factor of 300–500 and completely blocks the FID signal in the absence of the magnetic field. In the magnetic field, the polarization of the FID depends on time, and the vertical polarization of the FID could be observed. A short incident laser pulse partially reached the detector and formed some spurious signal. This signal was accumulated separately with an empty cell and subtracted from the experimental signals.

3. Numerical simulation

Before starting a detailed description of the calculations, we will make a qualitative picture of the non-Faraday rotation of the FID. Let's imagine a single absorption line corresponding to the transition between the states with J and $J+1$. Short laser pulse creates a superposition of these lower and upper states and this nonstationary state emits FID radiation as long as the phase coherence exists. If polarization of the laser pulse is linear, polarization of the FID is linear too. In a longitudinal magnetic field absorption line splits into two components σ^+ and σ^- corresponding to transitions $\Delta M_J = 1$ and $\Delta M_J = -1$. The linearly polarized laser pulses can be presented as a superposition of two pulses with the right-hand circular and left-hand circular polarization. The right-hand circular polarized pulse creates a superposition of the lower and upper states according to $\Delta M_J = 1$ selection rule and the left-hand circular polarized pulse according to $\Delta M_J = -1$. These superpositions emit right-hand circular polarized FID and left-hand circular polarized FID with slightly different frequencies due to Zeeman splitting. After combination of two circular polarized waves with slightly different frequencies we will get linear polarized wave which plane of polarization depends on time.

These qualitative considerations mean that in a longitudinal magnetic field we expect rotation of the polarization plane of the FID. The speed of rotation corresponds to the Zeeman splitting and for a long-lived FID signal, the angle can be big. The rotation angle of the FID depends only on spectroscopic parameters of individual molecule in contrast with ordinary Faraday effect, where rotation angle depends on molecule concentration.

The numerical simulation mostly follow the described qualitative scheme. The difference is that even in the absence of a magnetic field, we are dealing with the splitted absorption line. Another complication arises from the large number σ^+ and σ^- components because of different sensitivity to magnetic field of lower and upper states.

All the experiments were made at the absorption lines of NO that correspond to the transition $J = 18.5 \rightarrow J = 19.5$ in the ground electronic state. Both lower and upper rotational states have two spin–orbit components with $\Omega = 3/2$ and $\Omega = ½$. Each component has a small Λ-doublet splitting and hyperfine splitting. Hyperfine splitting is <1 MHz and could be neglected in our experiments. Therefore the rotation states are split into four components. The frequencies of absorption lines [25] are listed in the Table 1.

The magnetic field causes the splitting of rotational levels by the projection of the total angular momentum M_J. In the small field, splitting is linearly dependent on the magnetic field

$$\Delta E = g_{J,\Omega}\beta H \cdot M_J \tag{1}$$

where $g_{J,\Omega}$ is g-factor of the rotational state of total moment J and projection of electronic moment Ω, β is Bohr magneton, H is magnetic field. The values of g-factors were calculated using the formulas from [26].

In the presence of the longitudinal magnetic field, selection rules are $\Delta M_J = \pm 1$. Signs '+' and '−' correspond to the right-hand and left-hand circular polarization (σ^+ and σ^-). According to (1), the absorption line should split into 76 components in the magnetic field: 38 with σ^+ polarization and 38 with σ^- polarization. The splitting of lines $\Omega = 3/2$ and $\Omega = ½$ in the magnetic field of 720 G is shown in the upper part of Figure 1. The solid line in the figure shows the total shape of absorption line arising due to collision broadening. The width of the individual line was set 8 MHz, which corresponds to the pressure of several Torr [27]. NO pressure in experiments was varied within the range 2.5–10 Torr, therefore M_J – structure of absorption lines was unresolved. The bottom part of Figure 1 shows the total splitting of the absorption lines of $J = 18.5 \rightarrow J = 19.5$ transition into σ^+ and σ^- components. In both cases Zeeman splitting is less than Λ-doubling. The spectral width of the laser is 0.2 cm^{-1}. Therefore the laser spectra can overlap four lines near 65.17 cm^{-1} or four lines near 66.80 cm^{-1}.

Note that calculation predicts larger splitting of the $\Pi_{1/2}$ term than that of $\Pi_{3/2}$. This conclusion is somewhat unexpected, as the states of the $\Pi_{1/2}$ term are often considered magnetically insensitive due to the compensation of spin and orbital magnetic moments [28]. This is because for NO molecule the Hund's case **a** does not work well for big values of J.

The next step in numerical simulation is calculation of the FID signal depending on time $F(t)$. Linearly polarized incident laser pulse $E(t)$ was presented as a superposition of right-hand and left-hand circular polarized terms.

$$E_x(t) = E^+(t) + E^-(t)$$

Then the right-hand and left-hand circular polarized FID signals were calculated separately. Calculation procedure is described in [28]. In the calculations, the contributions of all 76 absorption lines with $\Delta M = +1$ or all lines with $\Delta M = -1$ were taken into account. As a result of calculations, two complex functions $F^+(t)$ and $F^-(t)$ were obtained. These functions describe the amplitude and the phase of right-hand and left-hand circular polarized waves. The total FID signal was obtained by summation of these circular polarized waves. It can be shown that the following formula is valid for the intensity of the FID polarized as the incident laser pulse:

$$I_x(t) = \left|F^+(t) + F^-(t)\right|^2 \tag{2}$$

The similar formula for the intensity of the perpendicular polarized FID is:

$$I_y(t) = \left|F^+(t) - F^-(t)\right|^2 \tag{3}$$

And the angle of rotation of the polarization plane of FID can be calculated using:

$$tg(2\varphi) = \frac{Im(F^+(t)^* \cdot F^-(t))}{Re(F^+(t)^* \cdot F^-(t))}, \tag{4}$$

where the asterisk denotes complex conjugation.

Table 1
Frequencies of the absorption lines of NO and g-factors of the corresponding rotation states. Letters 'e' and 'f' denote Λ-doublet components.

Line assignment	Line positions	g Factor of the lower state	g Factor of the upper state
$^2\Pi_{1/2}(19.5 \leftarrow 18.5)_e$	65.1661 cm^{-1}	0.025841	0.025537
$^2\Pi_{1/2}(19.5 \leftarrow 18.5)_f$	65.1735 cm^{-1}	0.025841	0.025537
$^2\Pi_{3/2}(19.5 \leftarrow 18.5)_e$	66.7993 cm^{-1}	−0.0165262	−0.0170329
$^2\Pi_{1/2}(19.5 \leftarrow 18.5)_f$	66.8037 cm^{-1}	−0.0165262	−0.0170329

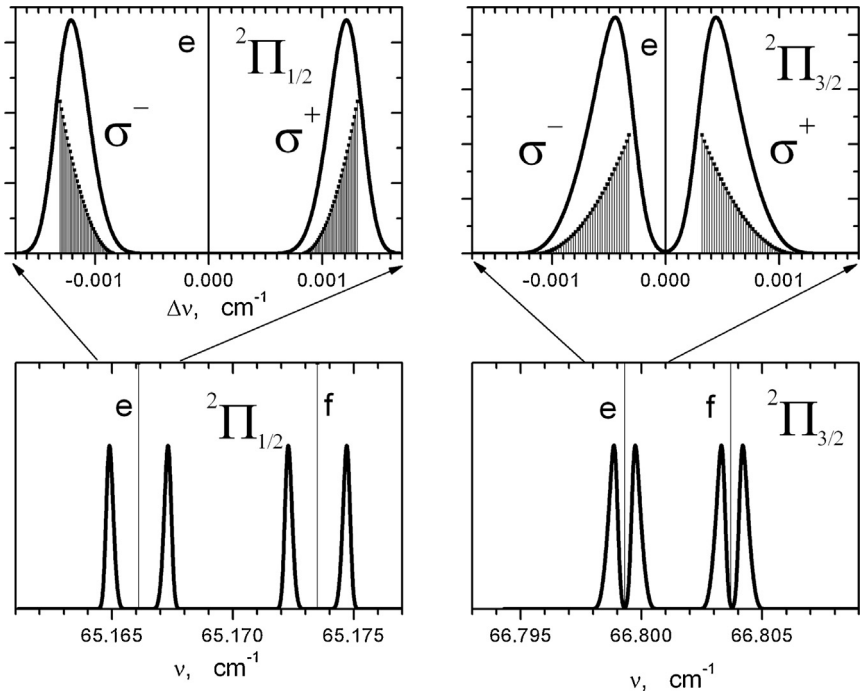

Figure 1. Splitting of the $J = 18.5 \rightarrow J = 19.5$ absorption lines of NO in magnetic field 720 G. Bottom panels show total spectra. Letters 'e' and 'f' mark the position of Λ-doublet components. Upper panels show splitting of individual lines in magnetic field. M_J-structure is unresolved due to the collision broadening.

4. Experimental results

The signals observed for $^2\Pi_{3/2}$ states at 66.8 cm^{-1} are shown in Figure 2. The upper panel shows FID signal in NO, recoded in preliminary experiment without magnetic field and polarizer. The oscillations of the FID signal correspond to Λ – doublet splitting of absorption line 0.0044 cm^{-1}. Numerical modeling of the FID (blue dashed line) based on the data in Table 1 coincides exactly with the experimental signal.

The lower panel shows the signals recorded after installing the polarizer. Without magnetic field, the polarization of the FID is linear, and the polarizer after the sample completely blocks the signal. In the magnetic field, the plane of FID polarization depends on time. Immediately after the laser pulse, the FID polarization is the same as laser polarization. With time after the pulse, polarization of the FID rotates, and radiation comes to the detector.

The signals observed for another electronic state $^2\Pi_{1/2}$ are shown in Figure 3. Like in the previous case, in the zero magnetic field the polarizer completely blocks FID. In nonzero magnetic field FID reaches the detector due to the rotation of the polarization plane. The period of oscillations is shorter because Λ – doublet splitting for this state is larger (0.0074 cm^{-1}).

Figure 4 shows the signals at $^2\Pi_{1/2}$ state observed in different magnetic field: 720 G and 360 G. The period of oscillations does not depend on magnetic field, which confirms their origin from the Λ-doublet splitting. The upper part of Figure 4 presents numerical modeling of the FID using formula (3). For $H = 360$ G the simulated and experimental signals are in good agreement. For $H = 720$ G the agreement is good at $t < 12$ ns but at $t > 20$ ns the agreement becomes poor, numerical calculation predicts the signal that was not observed in experiment.

The speed of rotation of the FID polarization depends on magnetic field. This fact is clearly visible from the comparison of experimental curves in Figure 4. The maximum of the experimental curve approximately corresponds to the moment when the rotation angle is 90 degrees. In the field of 720 G this happens in 8–10 ns after the laser pulse, whereas in the field of 360 G polarization rotates slower and this moment comes in 13–15 ns. Such estimations from the peak position are very approximate because they ignore the exponential decay of the FID over time. More accurate values of the rotation angle can be obtained from simulation. Figure 3 shows the polarization rotation angle of the FID, calculated using formula (4) in the field of 720 G. Simulation shows that the rotation angle reaches 180° at a time $t = 18$ ns. At this point, the signal should vanish, and upon further rotation reappear (the upper part of Figure 4). In the experiment, the increase of the signal again after 180° rotation could not be observed due to the high magnetic field inhomogeneity along the length of the gas cell. At low magnetic field the rotation angle does not exceed 180° for the whole time of signal decay.

In modeling the observed signals, we do not change any spectroscopic parameters except for the width of the absorption lines. Under our experimental conditions, the width of the absorption lines is determined by collision broadening. Broadening constants for NO – NO collisions are available in [27] and are equal to 2.16 and 2.35 MHz/Torr for the lines at 65.17 cm^{-1} and 66.8 cm^{-1}, respectively. To obtain agreement with the experimental signals, we had to increase the value of the broadening constants significantly to

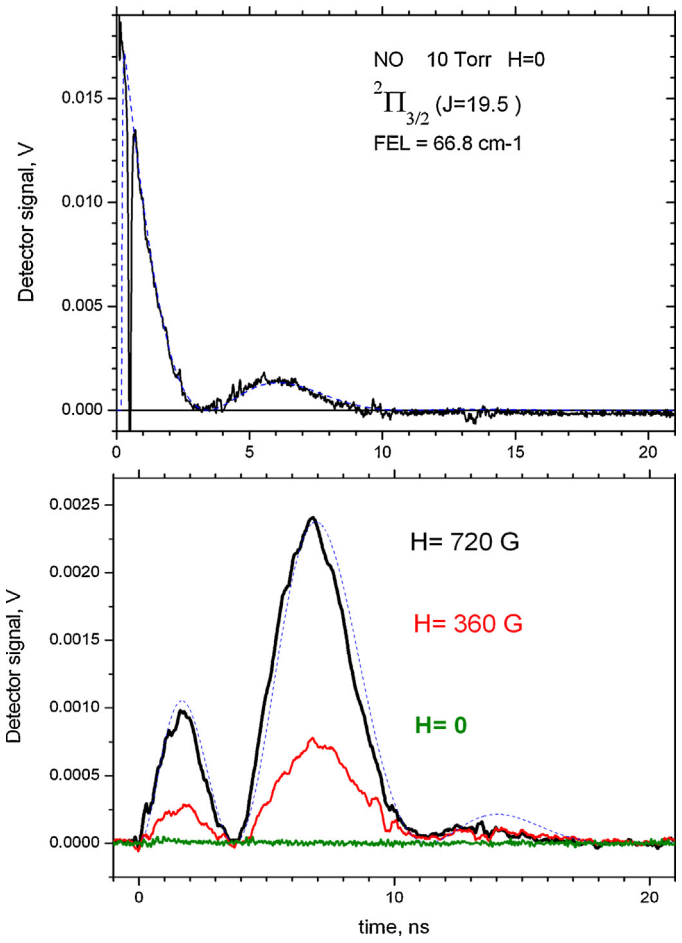

Figure 2. Experimental signals at 66.8 cm^{-1} for $^2\Pi_{3/2}$ state. Upper panel – Preliminary measurements of the FID at zero magnetic field without polarizer. Lower panel – FID signals at $H = 0$, $H = 360$ G and $H = 720$ G recorded with polarizer. Blue dash line – numerical modeling for both lower and upper panels. (For interpretation of the references to color in this figure legend, the reader is referred to the web version of this article.)

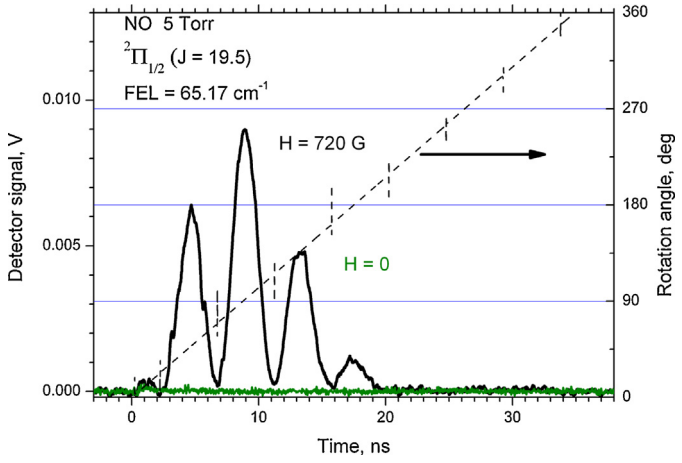

Figure 3. Experimental signals at 65.17 cm^{-1} for $^2\Pi_{1/2}$ state at $H = 0$ and $H = 720$. Dash line shows the polarization rotation angle of the FID.

approximately 7–10 MHz/Torr. A possible explanation for this difference is that literature values are given in the absence of the magnetic field. In the magnetic field, the absorption lines are spilt, and broadening of the split components can occur in collisions that do not lead to broadening of the nonsplit line.

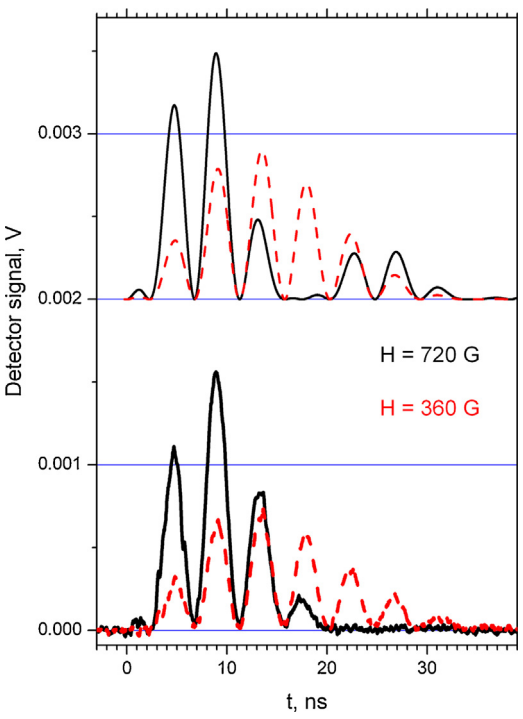

Figure 4. Experimental signals at 65.17 cm^{-1} for $^2\Pi_{1/2}$ state at different magnetic field. Lower part – experiment. Solid black line – $H = 720$ G, red dash line – $H = 360$ G. Upper part – numerical simulation. (For interpretation of the references to color in this figure legend, the reader is referred to the web version of this article.)

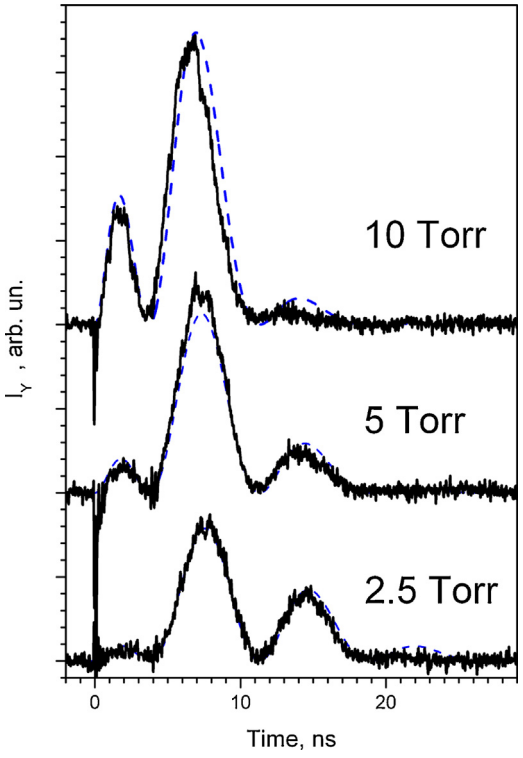

Figure 5. Experimental FID signals (solid black) for $^2\Pi_{1/2}$ state at different pressures of NO. Laser 66.8 cm^{-1}. $H = 720$ G. Dash – blue lines – simulation. Width of the lines 10 Torr – 70 MHz; 5 Torr – 45 MHz; 2.5 Torr – 30 MHz. (For interpretation of the references to color in this figure legend, the reader is referred to the web version of this article.)

A qualitative picture of the effect of pressure on the observed signal is shown in Figure 5. The dependence of the signal on time is determined by two factors. The first factor is the rotation of the plane of polarization, which increases linearly with time after the pulse. Another factor is the exponential decay of the FID signal. At high pressure the exponential decay is fast and only the initial part of the signal is observed. At low pressure it is possible to observe the later part of FID that has an advantage over the initial part due to the larger rotation angle. Separate oscillations of the signal are associated with Λ-doubling and their positions do not depend on the magnetic field or gas pressure.

It will be useful to discuss the relationship of the observed effect with the conventional Faraday effect. A characteristic feature of the Faraday effect is an increase in the rotation angle with the concentration of gas molecules. In contrast, the rotation of FID polarization does not depend on concentration and is much bigger than Faraday rotation. Therefore it is called 'non-Faraday' rotation [4]. To identify the close connection between these two phenomena the input continuous wave can be presented as a sequence of short pulses. Each short linearly polarized pulse after propagating through a medium in the magnetic field will give a short pulse and a weak FID signal. The polarization of the short output pulse coincides with the polarization of the input pulse, but FID polarization depends on time. Averaging all of the output waves, will get continuous electromagnetic wave with a small angle of rotation of the polarization plane that is equivalent to the ordinary Faraday effect. Moreover, this small angle will increase with the concentration of molecules, because the amplitude of the FID increases. This means that the difference between conventional Faraday effect and 'non-Faraday rotation' of the FID arises from the use of short pulses and real-time monitoring.

Acknowledgements

This work was supported partly (special stabilized regimes of the NovoFEL and ultrafast equipment) by Russian Science Foundation (project 14-50-00080) and partly (gas and magnetic field systems, and experimental setup) by Russian Foundation for Basic Research (project 15-03-05352 A).

References

[1] R.G. Brewer, R.L. Shoemaker, Phys. Rev. A 6 (1972) 2001.
[2] E.N. Chesnokov, V.V. Kubarev, P.V. Koshlyakov, Appl. Phys. Lett. 105 (26) (2014) 261107.
[3] V.G. Gol'dort, D.V. Ledovskikh, E.B. Khvorostov, N.N. Rubtsova, Laser Phys. Lett 5 (3) (2008) 197.
[4] N.N. Rubtsova, I.V. Yevseeyev, Laser Phys. 17 (2007) 244.
[5] J.P. Gordon, C.H. Wang, C.K.N. Patel, R.E. Slusher, W.J. Tomlinson, Phys. Rev. 179 (1969) 294.
[6] E.N. Chesnokov, V.V. Kubarev, P.V. Koshlyakov, G.N. Kulipanov, Laser Phys. Lett. 10 (5) (2013) 055701.
[7] G. Litfin, C. Pollock, R. Curl, F. Tittel, J. Chem. Phys. 72 (1980) 6602.
[8] H. Sabana, T. Fritsch, M. Boyomo Onana, O. Bouba, P. Hering, M. Murtz, Appl. Phys. B 96 (2009) 535.
[9] M. Koch, X. Luo, P. Murtz, W. Urban, K. Morike, Appl. Phys. B 64 (6) (1997) 683.
[10] H. Ganser, W. Urban, A.M. Brown, Mol. Phys. 101 (4–5) (2003) 545.
[11] T. Fritsch, M. Horstjann, D. Halmer, P. Sabana, P. Hering, M. Murtz, Appl. Phys. B 93 (2–3) (2008) 713.
[12] R. Lewicki, J.H. Doty 3rd, R.F. Curl, F.K. Tittel, G. Wysocki, Proc. Natl. Acad. Sci. U. S. A. 106 (31) (2009) 12587.
[13] C.A. Zaugg, R. Lewicki, T. Day, R.F. Curl, F.K. Tittel, Faraday rotation spectroscopy of nitrogen dioxide based on a widely tunable external cavity quantum cascade laser, in: Proc. SPIE 7945, Quantum Sensing and Nanophotonic Devices VIII, 79450O (January 24, 2011), 2011.
[14] J.M. Smith, J.C. Bloch, R.W. Field, J.L. Steinfeld, J. Opt. Soc. Am. B 12 (6) (1995) 964.
[15] W. Dillenschneider, R.F. Curl Jr., J. Mol. Spectrosc. 99 (1) (1983) 87.
[16] C. Pfelzer, M. Havenith, M. Peric, P. Mürtz, W. Urban, J. Mol. Spectrosc. 176 (28) (1996).
[17] J. Pfeiffer, D. Kirsten, P. Kalkert, W. Urban, Appl. Phys. B 26 (3) (1981) 173.
[18] W. Zhao, G. Wysocki, W. Chen, E. Fertein, D. Le Coq, D. Petitprez, W. Zhang, Opt. Express 19 (3) (2011) 2493.
[19] R.J. Brecha, L.M. Pedrotti, D. Krause, J. Opt. Soc. Am. B 14 (8) (1997) 1921.
[20] S.G. So, E. Jeng, G. Wysocki, Appl. Phys. B 102 (27) (2011) 9–291.
[21] J. Shao, L. Lathdavong, J. Westberg, P. Kluczynski, S. Lundqvist, O. Axner, Appl. Opt. 49 (29) (2010) 5614.
[22] E.N. Chesnokov, O.S. Aseev, O.P. Korobeinichev, et al., Combust. Explos. Shock Waves 46 (2) (2010) 149.
[23] N.G. Gavrilov, et al., Nucl. Instrum. Methods A 575 (54) (2007).
[24] V.V. Kubarev, V.K. Ovchar, K.S. Palagin, Ultra-fast terahertz Schottky diode detector, in: Conference Digest of the 34th International Conference on Infrared, Millimeter and Terahertz Wave, Busan, Korea, 21–25 September, 2009, 2009.
[25] T.D. Varberg, F. Stroh, K.M. Evenson, J. Mol. Spectrosc. 196 (1) (1999) 5–13.
[26] M. Mizushima, K.M. Evenson, J.S. Wells, Phys. Rev. A 5 (1972) 2276.
[27] A. Goldman, L.R. Brown, W.G. Schoenfeld, M.N. Spencer, C. Chackerian Jr., L.P. Giver, et al., J. Quant. Spectrosc. Radiat. Transfer 60 (1998) 825.
[28] J.M. Brown, A. Carrington, Rotational Spectroscopy of Diatomic Molecules, Cambridge University Press, Cambridge, 2003.
[29] E.N. Chesnokov, V.V. Kubarev, P.V. Koshlyakov, G.N. Kulipanov, Appl. Phys. Lett. 101 (2012) 131109.